TÜBİTAK

Turkish Journal of Earth Sciences

http://journals.tubitak.gov.tr/earth/

Research Article

Turkish J Earth Sci
(2021) 30: 916-927
© TÜBİTAK
doi:10.3906/yer-2105-38

Quantifying the bathymetric stripping gravity corrections of global seawater and major lakes over Turkey

Mehmet SİMAV*, **Hasan YILDIZ**
General Directorate of Mapping, Ankara, Turkey

Received: 25.05.2021 • **Accepted/Published Online:** 01.09.2021 • **Final Version:** 22.11.2021

Abstract: Gravity data inversion or interpretation requires the removal of the gravitational effects of the a priori known geologic and/or morphologic features within the Earth's system to model and reveal the remaining signals of the unknown anomalous subsurface density distributions. The Bouguer gravity anomalies reduced by the normal gravitational field of the Earth and the gravitational attraction of the topographic masses above the sea level are frequently used in geophysics for this purpose. However, density contrast effects of the other major known elements, such as offshore seawater, inland water bodies, glaciers, and/or sediments can be removed from the Bouguer gravity anomalies, which is denoted as stripping in gravimetry, to unmask the remaining gravitational signal of the sought anomalous masses. Stripping the Bouguer anomaly off seawater density contrast has become possible with the releases of freely available high-resolution global ocean bathymetry data. Moreover, the bathymetry data from recent hydrographic surveys over the inland water bodies with high-precision echo sounders has given rise to the opportunity to determine the stripping effects of the lake water density contrast. In this study, we quantify the global seawater bathymetry stripping effects along with lake water stripping of some greatest Turkish lakes on a regular 1' × 1' grid at the Earth's surface over Turkey including offshore. The seawater bathymetric corrections vary from 132 to 418 mGal over the seas and show a long-wavelength pattern over the inland with a mean value of 133 mGal. It produces significant variations onshore close to the coasts and on some islands up to 163 mGal. Although the bathymetric gravity stripping due to the lake water density contrast has negligible effects on their surrounding land areas, the water masses can produce notable effects on the lake surfaces reaching up to few tens of mGals at their deepest area, which should be considered in the microgravimetry studies over the lakes.

Key words: Global seawater bathymetric stripping, lake water bathymetric stripping, gravity anomaly, forward modelling, Turkey

1. Introduction

The Earth's gravity field described by Newton's universal law of gravitation mirrors the density structure, mass distribution, and dynamics of the Earth's interior (Hinze et al., 2013). Inversion of gravity field data lets geoscientists map out the subsurface geology, identify potentially favorable regions for resource exploration, and contribute substantially to the development of crust-mantle models, detection of tectonic structures, continental grabens, deep-sea trenches, oceanic ridges, and swells (Hinderer et al., 1991; Groten and Becker, 1995; Mazzotti et al., 2011; Tenzer et al., 2012a; Hwang et al., 2014; Sandwell et al., 2014; Reguzzoni and Sampietro, 2015; van der Meijde et al., 2015).

The gravity field measurements on or above the Earth's surface contain the combined effects of instrumental plus temporally and spatially varying gravitational attractions of extraterrestrial bodies, surface, terrain, atmospheric and subsurface masses. Depending on the application, some of these sources may be regarded as extraneous effects which mask or distort the anomalies under consideration. The unwanted extraneous effects are removed from the gravity data before the inversion or interpretation process to isolate the target sources. Time-variable instrumental and gravitational effects due to the solid Earth and ocean tides, atmospheric mass movements, polar motion, groundwater, and soil moisture variations are removed from the raw gravity data to obtain the actual static gravity field (Torge, 1989; Timmen, 2010; Simav and Yildiz, 2019). Then the actual static field can be transformed into the anomalous or disturbing field by introducing a reference normal gravity field generated by a suitable ellipsoid of revolution which captures the general features of the actual field (Heiskanen and Moritz, 1967; Bomford, 1971). There are several types of gravity anomalies defined in the anomalous gravity field (actual minus normal fields) based

* Correspondence: mehmet.simav@harita.gov.tr

This work is licensed under a Creative Commons Attribution 4.0 International License.

on the additional corrections applied for the extraneous sources. All anomalies have specific uses, but the complete Bouguer anomaly, which takes into account the correction for the gravitational attraction of the topographic masses above the sea level, is the most useful one in exploration geophysics and geodesy (Vaníček et al., 2001; Hinze et al., 2005; Vajda et al., 2006; Kuhn et al., 2009; Vajda et al., 2020). However, the Bouguer anomaly may still contain unwanted effects in practice. Density contrast effects of the other major known elements, such as atmosphere, offshore seawater, inland water bodies, glaciers, and/or sediments can be removed from the Bouguer gravity anomalies to unmask the remaining gravitational signal of the sought anomalous masses and isolate the targets of interest. In geophysics, this step is denoted as gravity stripping (Vajda et al., 2008), and this procedure is known to be more accurate than any other mathematical methods (e.g., convolution, filtering) for the separation of the gravity field signals (Simeoni and Brueckl, 2009; Bielik et al., 2013).

Ocean bathymetry-generated gravitational field quantities are computed by Tenzer et al. (2008a, 2008b), Tenzer et al. (2009), Tenzer et al. (2010), Novák (2010), Tenzer and Novák (2012b) globally based on spherical harmonic analysis and synthesis of the gravity field. Tenzer et al. (2009) computed the bathymetric stripping effects by utilizing 5' × 5' arc-min resolution Earth global topography and bathymetry data (ETOPO5) to generate the global bathymetric spherical harmonic model first, and subsequently compute the bathymetric stripping effect globally at the 1° × 1° arc-degree equiangular grid on the Earth's surface using the harmonic coefficients. Their results revealed that a significant amount of the gravitational signal is caused by the mean ocean density contrast (1640 kg/m^3) relative to the adopted mean crust density of Earth (2670 kg/m^3). They showed that seawater stripping corrections vary from 129 to 753 mGal with the mean of 327 mGal globally, where the maxima are located above the oceanic trenches and the minima in the central parts of the continental regions. Mikuška et al. (2006) studied the far-zone ocean bathymetry effect on gravity and concluded that ignoring the gravitational effects of distant bathymetry beyond the outer limit of the Hayford-Bowie zone O (approximately 1.5° and greater) would result in errors ranging from 128 to 225 mGal. Tenzer et al. (2012c) reevaluated the ocean bathymetric stripping effects globally again, but this time using depth-dependent seawater density model instead of mean density in the forward modeling. They found that the approximation of the actual seawater density by its mean value yields a relative error up to about 2% which reaches its maximum value of about 16 mGal, particularly over the deepest oceans. Moreover, Novák (2010) computed the gravitational potential of the ocean masses and Tenzer and Novák (2012b) evaluated the bathymetric stripping corrections to gravity gradient components. Although these studies provided interesting insights into the impact of seawater stripping effects on gravity, they are all derived from low-resolution ocean bathymetry data and evaluated globally on a very coarse grid resolution. To the best of our knowledge, there exists no rigorous publication for regional evaluation surrounding Turkey with higher computational grid resolution. Besides, the ocean bathymetry models have evolved during the last few years with the recent data from shipboard soundings and satellite altimetry observations. With these issues in mind, the first goal of this study is to compute the bathymetric stripping gravity corrections of global seawater on a regular 1' × 1' arc-min grid at the Earth's surface over the territory of Turkey including offshore bounded by 25°E–45°E and 35°N–43°N using the state-of-the-art SRTM15+ Shuttle Radar Topography Mission global bathymetry and topography model (Tozer et al., 2019).

The second goal of this study is to evaluate the lake bathymetry stripping effects over the same region and at the same computation points which have not been studied in Turkey so far. There are many natural and man-made inland water bodies covering a surface area of about 11,000 km^2 in Turkey. The Turkish General Directorate of Water Management has been surveying the depth of inland waters with Global Navigation Satellite System (GNSS)-aided high-precision echo sounders steadily. The bathymetry data of the largest and deepest five lakes are used to quantify the stripping effects of the lake water density contrast for the first time.

Section 2 describes the methodology and presents the expressions for computing the global seawater and lake bathymetry gravity stripping corrections. The third part explains the data used in the study. Section 4 presents and evaluates the results. The summary and conclusions are given in Section 5.

2. Methodology

Newton's volume integral for the gravitational attraction of bathymetric density contrast along the radial or vertical direction (A^{BDC}) can be written in spherical coordinates as follows (Vajda et al., 2004):

$$A^{BDC}(\varphi_P,\lambda_P,r_P) = -G\int_{\varphi_Q=-90^\circ}^{\varphi_Q=+90^\circ}\int_{\lambda_Q=-180^\circ}^{\lambda_Q=+180^\circ}\int_{r_Q=r_1}^{r_Q=r_2}\Delta\rho(\varphi_Q,\lambda_Q,r_Q)\frac{\partial L^{-1}}{\partial r_Q}r_Q^2\cos(\varphi_Q)\,dr_Q\,d\lambda_Q\,d\varphi_Q \quad (1)$$

where subscripts P and Q denote the computation point and running or integration points, respectively. The coordinate triplet (φ, λ, r) represents the spherical latitude, longitude,

and radius where r is the sum of Earth's mean radius (R = 6371 km) and the point height above sea level. G = 6.674 × 10^{-11} $m^3kg^{-1}s^{-2}$ is the Newton's gravitational constant, and L is the Euclidean spatial distance between computation and integration points where ψ_{PQ} is a spherical distance which can easily be computed using the law of cosines as follows:

$$L = L(\varphi_P, \lambda_P, r_P, \varphi_Q, \lambda_Q, r_Q) = \sqrt{r_P^2 + r_Q^2 - 2r_P r_Q \cos(\psi_{PQ})} \quad (2)$$

$$\cos(\psi_{PQ}) = \cos(\varphi_P)\cos(\varphi_Q) + \sin(\varphi_P)\sin(\varphi_Q)\cos(\lambda_P - \lambda_Q) \quad (3)$$

The variable $\Delta\rho(\varphi_Q, \lambda_Q, r_Q)$ is the bathymetric density contrast at the integration point. Assuming a constant crustal density of 2670 kgm^{-3}, seawater density of 1025 kgm^{-3}, and fresh/alkaline water density of 1000 kgm^{-3}, the bathymetric density contrast is the difference between crustal and water density which yields $\Delta\rho$ = 1645 kgm^{-3} for seawater and $\Delta\rho$ = 1670 kgm^{-3} for fresh/alkaline waters. Eq. (1) can be rewritten for the constant density as follows where the innermost integration limits are equal to $r_1 = R - H^{\text{Sea Depth}}$ and $r_2 = R$ for ocean bathymetry, and $r_1 = R + H^{\text{Lake Floor}}$ and $r_2 = R + H^{\text{Lake Surface}}$ for lake bathymetry. H corresponds to the depth and height below and above sea level.

$$A^{BDC}(\varphi_P, \lambda_P, r_P) = -G\Delta\rho \int_{\varphi_Q=-90^\circ}^{\varphi_Q=+90^\circ} \int_{\lambda_Q=-180^\circ}^{\lambda_Q=+180^\circ} \int_{r_Q=r_1}^{r_Q=r_2} \frac{\partial L^{-1}}{\partial r_Q} r_Q^2 \cos(\varphi_Q) dr_Q d\lambda_Q d\varphi_Q \quad (4)$$

The volume integral in Eq. (4) can be evaluated in space or frequency domains either by direct integration or spherical harmonic methods (Kuhn and Seitz, 2005; Wild-Pfeiffer and Heck, 2007; Wild-Pfeiffer, 2008). Numerical evaluation in the space domain relies upon a mass discretization because the geometry of mass bodies is only available in the discrete form represented by a grid with a specific resolution in practice. The integration domain can be decomposed into elementary geometrical bodies such as polyhedra, prisms, tesseroids, point masses, mass lines, and/or mass layers (Nagy et al., 2000; Wild-Pfeiffer, 2008; Tsoulis, 2012; Grombein et al., 2013; D'Urso, 2013; Uieda et al., 2016), then the superposition principle can be applied to sum up the effects of all individual mass bodies.

The triple integral can also be evaluated numerically using the quadrature methods e.g., the 3D Gauss–Legendre cubature (Asgharzadeh et al., 2007). Another possibility is the decomposition of the elliptic integral into a one-dimensional integral over the radial parameter r_Q for which an analytical solution exists, then 2D spherical integral can be solved by quadrature methods. The radial integration of the radial derivative of the reciprocal spatial distance $\partial L^{-1}/\partial r_Q$ multiplied by r^2_Q can be expressed analytically as follows (Novák, 2000):

$$K = \int_{r_Q=r_1}^{r_Q=r_2} \frac{\partial L^{-1}}{\partial r_Q} r_Q^2 \, dr_Q$$

$$= \left| \frac{(3r_P^2 + r_Q^2)\cos(\psi_{PQ}) + r_P r_Q (1 - 6\cos^2(\psi_{PQ}))}{L} + r_P(3\cos^2(\psi_{PQ}) - 1)\ln|r_Q - r_P\cos(\psi_{PQ}) + L| \right|_{r_Q = r_1}^{r_Q = r_2} \quad (5)$$

In general, the bathymetry or topography data are stored on a regular grid resolution $\Delta\lambda$ in longitude and $\Delta\varphi$ in latitude. The single quadrature formula for such uniform grid yields attraction of constant bathymetric density contrast as follows:

$$A^{BDC}(\varphi_P, \lambda_P, r_P) = -G\Delta\rho \sum_j K_j \cos(\varphi_{Q_j}) \Delta\lambda\Delta\varphi \quad (6)$$

The summation in Eq. (6) is evaluated over discrete values of the kernel function K_j that corresponds to the computation point (φ_P, λ_P, r_P) and the center of the j^{th} geographical cell defined in terms of its center (φ_{Qj}, λ_{Qj}) and its average depth and/or height. We use the scheme given in Eq. (6) and implemented it in MATLAB to compute the bathymetric stripping gravity effects. Investigations on the other numerical evaluation methods of Eq. (4) by elementary geometrical bodies or 3D integration are out of the scope of this study.

3. Data

3.1. ASTER global digital elevation model

ASTER stands for Advanced Spaceborne Thermal Emission and Reflection Radiometer onboard the NASA's Terra spacecraft which collects high-resolution images of the Earth in different bands of the electromagnetic spectrum. Using the stereo pairs provided by the ASTER instrument, the Ministry of Economy, Trade and Industry of Japan (METI) and NASA produce high-resolution and nearly global coverage of digital elevation model named ASTER GDEM. The model covers all the land surfaces between 83°N and 83°S with a spatial resolution of 1" × 1" arcsec. More information can be found at https://asterweb.jpl.nasa.gov/, https://earthdata.nasa.gov/learn/articles/new-aster-gdem, and https://ssl.jspacesystems.or.jp/ersdac/GDEM/E/1.html. The data is publicly available at https://gdemdl.aster.jspacesystems.or.jp/index_en.html and https://search.earthdata.nasa.gov/search/.

The study area extends from 25°E to 45°E in eastern longitudes and 35°N to 43°N in northern latitudes and shown in Figure 1 with a black rectangle comprises 577681 computation points separated on a regular 1' × 1' arc-min grid, 410756 of which are located on land and 166925 are offshore. Since the computations are done on the Earth surface, we use the latest version of ASTER GDEM data (V3) to extract the heights of 410756 land points within the study area. The heights of the offshore computation points are set to zero (e.g., on the sea surface). The statistics of the computation point heights are presented in Table 1.

3.2. SRTM15+ global bathymetry and topography

The SRTM15+ is global bathymetry and topography dataset which is an updated version of the SRTM+ series (Becker et al., 2009; Olson et al., 2016). It is distributed with a spatial resolution of 15" × 15" arcsec. We use the recently released version (V2.0) published by Tozer et al. (2019). The bathymetry data presented in the SRTM15+V2.0 dataset is produced using a combination of shipboard soundings and depths predicted from satellite altimetry. The data is publicly available and can be accessed from https://topex.ucsd.edu/WWW_html/srtm15_plus.html.

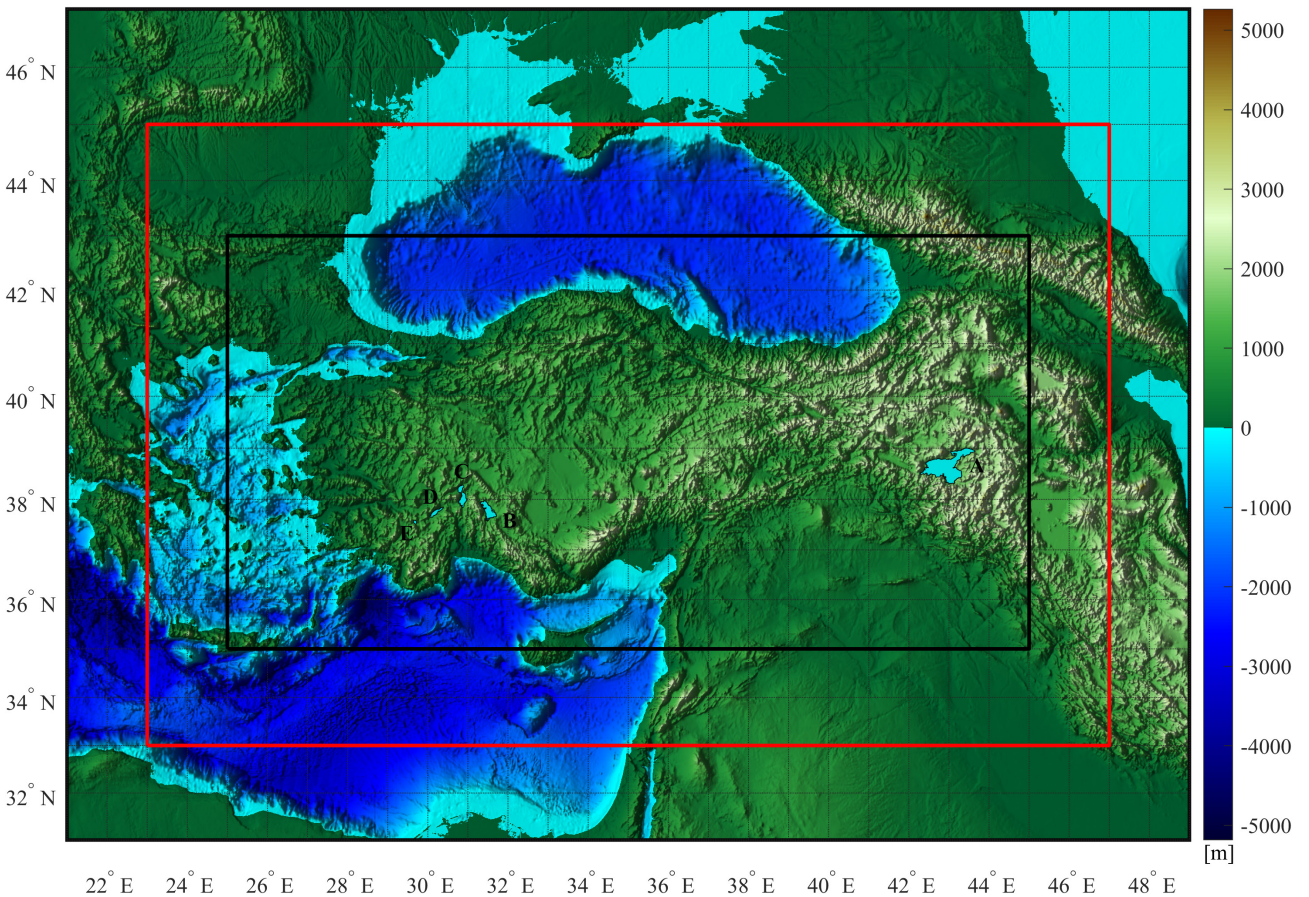

Figure 1. Topography and the bathymetry of the study region depicted with 15" arcsec resolution original SRTM15+ data. The black rectangle shows the study area. The red rectangle shows the extent of the near zone boundary. The five lakes considered in the study are also displayed with letters. (A) Lake Van, (B) Lake Beyşehir, (C) Lake Eğirdir, (D) Lake Burdur, and (E) Lake Salda.

Table 1. The statistics of the computation point heights and ocean bathymetry data for near and far zones. Units are in meters.

	Min	Max	Mean	Std
Computation point heights	0.0	5009.1	721.1	744.9
Near zone ocean bathymetry from 15" × 15" arcsec original SRTM15+ V2.0 data	–4560.0	0.0	–1431.9	979.1
Far zone ocean bathymetry from 15' × 15' arc-min block averaged SRTM15+ V2.0 data	–9874.4	0.0	–3454.8	1692.2

The integration domain for the ocean bathymetry stripping effect is split into two zones (near and far zones) in order to reduce computational costs. The 15" arcsec original SRTM15+ V2.0 data are used up to a spherical distance of 2° arc-degree from any computation point, and block average values of 15' arc-min data are used for the far zone (the remainder to the full globe) effects. Figure 1 shows extent of the near zone boundary with a red rectangle along with its topography and the bathymetry. Figure 2 displays the far zone ocean bathymetry. The statistics of the ocean bathymetry data for near and far zones are presented in Table 1.

3.3. Lake bathymetry

There are about 320 natural lakes and 861 man-made dams in Turkey varying greatly in size and depth (https://www.dsi.gov.tr/Sayfa/Detay/754#). Among them, we choose the four largest and one deepest lake with readily available bathymetry data. The first largest is the Lake Van located in eastern Turkey which covers more than 3700 km^2 surface area and has more than 600 km^3 water volume. It is also the largest alkaline lake on Earth with a maximum depth of about 450 m (Figure 3a). Although the Lake Tuz in central Turkey is the second largest lake in Turkey, it is not included in this study due to its very shallow depth of about 1 meter. The third and the fourth largest freshwater lakes namely the Lakes Beyşehir and Eğirdir are involved in the study. They are both located in a region called Lake District in south-western Turkey and cover more than 1100 km^2 surface area with mean depths of about 6–7 m (Figure 3b). The seventh-largest and third deepest Lake Burdur situated in the same region which has a surface area of about 200 km^2 is also considered in the study. It is a large saline and highly alkaline lake of tectonic origin with a maximum depth of about 70 m (Figure 3c). The last lake involved in the study is Lake Salda, a midsize crater lake positioned in the Lake District region. Although small in size (approximately 45 km^2 surface area), it is one of the deeper lakes (> 110 m) in Turkey (Figure 3c). National Aeronautics and Space Administration (NASA) reported in March 2021 that the minerals and rock deposits at the Lake Salda resemble to those around the Jezero Crater of Mars where the surface-exploring rover Perseverance was landed (https://en.wikipedia.org/wiki/Lake_Salda).

The bathymetry data of the lakes used in the study are provided by the Turkish General Directorate of Water Management. After screening and removing any outlying data, we regenerated 3" × 3" arcsec regular grids for each lake shown in Figure 3. Some more information about the lake bathymetry data is presented in Table 2.

4. Results

The bathymetric stripping corrections of constant global seawater density contrast ($\Delta\rho$ = 1645 kgm^{-3}) down to the ocean bottom are computed on a regular 1' × 1' arc-min geographical grid at the Earth's surface around Turkey. The results are shown in Figure 4. We display the corrections separately with different color bars for the offshore (Figure

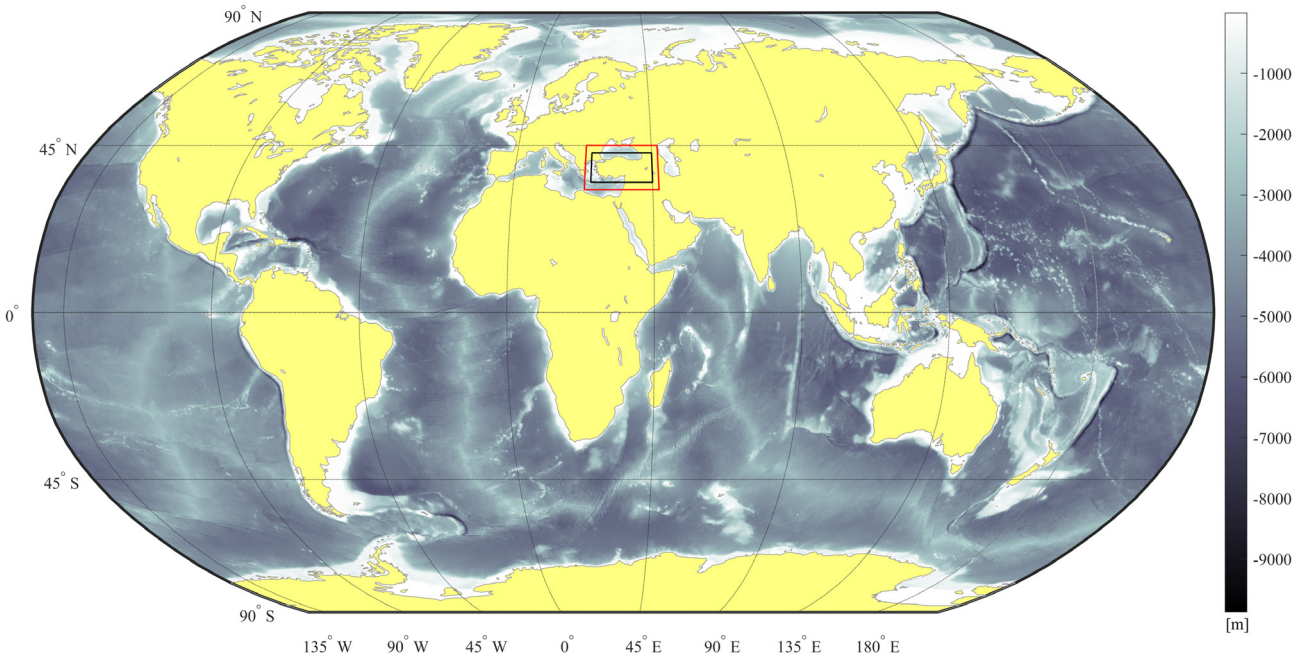

Figure 2. Far zone ocean bathymetry depicted with 15' arc-min block averaged SRTM15+ data. The black rectangle shows the study area. The red rectangle shows the extent of the near zone boundary.

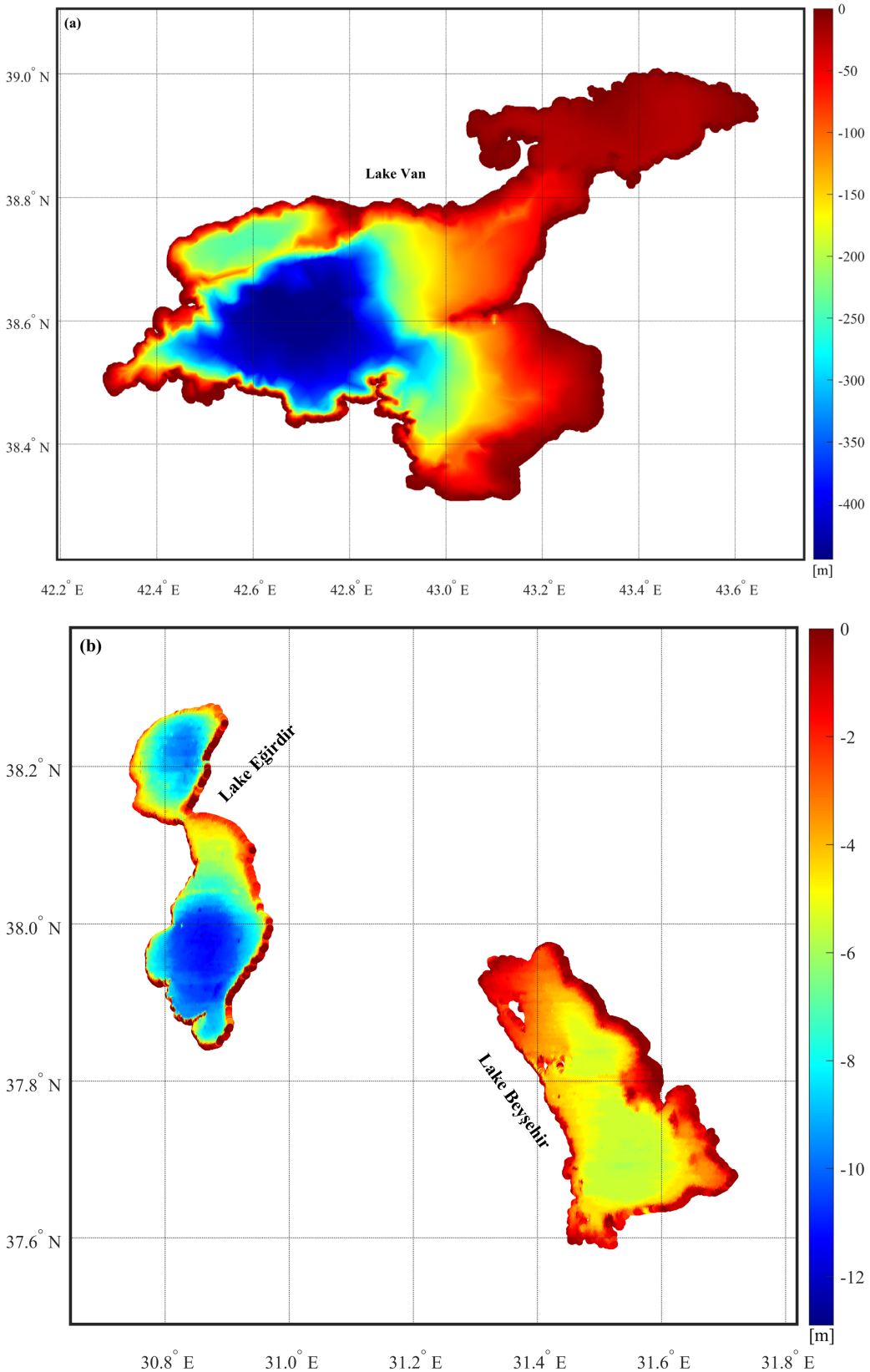

Figure 3. Lake floor bathymetries relative to the corresponding lake surfaces. (a) Lake Van, (b) Lakes Eğirdir and Beyşehir, (c) Lakes Burdur and Salda.

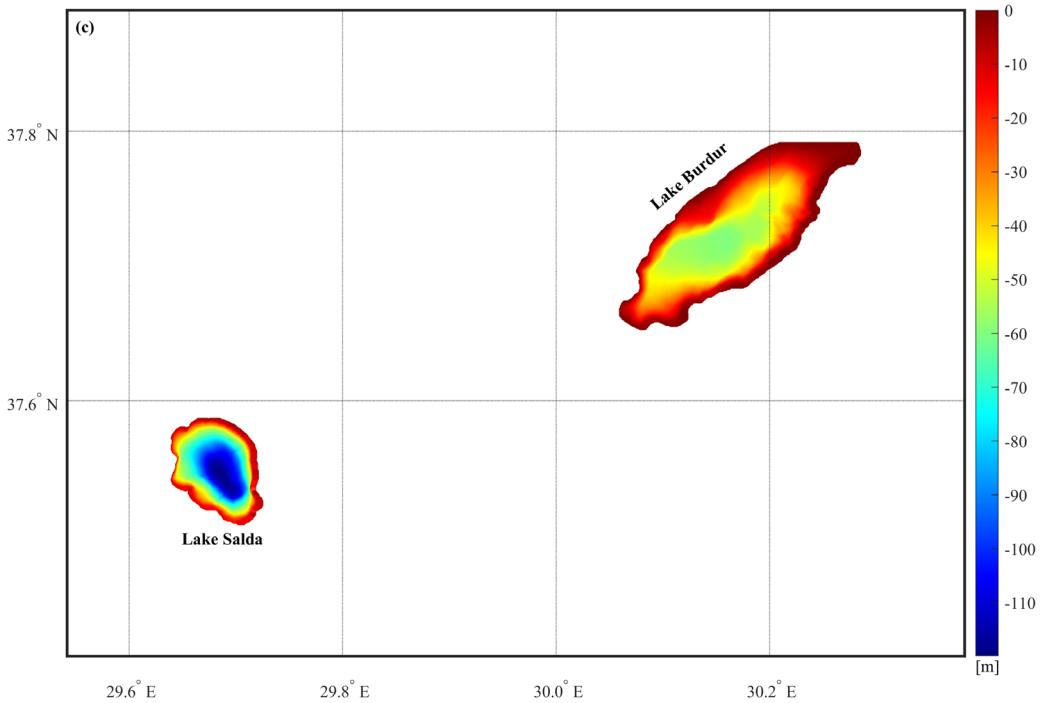

Figure 3. (Continued).

Table 2. Some numerical information about the five lakes used in the study.

Lake name	Van	Beyşehir	Eğirdir	Burdur	Salda
Max depth below lake surface (m)	–445.0	–6.1	–12.9	–60.3	–119.9
Mean depth below lake surface (m)	–159.8	–3.8	–7.7	–30.6	–66.5
Surface height above sea level (m)	1646.0	1121.0	917.6	841.0	1143.3
Surface area (km^2)	3574.4	636.2	455.5	141.7	43.5

4a) and onshore (Figure 4b) areas to easily distinguish and visualize the variations over the coastal regions and the islands. In the study region, the bathymetric correction varies from 132 to 418 mGal with a mean of 214 mGal and a standard deviation of 62 mGal over the marine areas (see Table 3). The variations of magnitude of the corrections are highly correlated with the ocean bathymetry and reveal the main structures of the ocean floor relief, as expected. The highest values are observed to the east of Rhodes island from which the Hellenic arc is passing (28.65°E and 35.93°N), and the offshore Gulf of Antalya. The corrections are mostly below the mean value in the Aegean Sea due to its relatively shallower bathymetry. In the Sea of Marmara, the corrections attain their maximum values up to 215 mGal over the Tekirdağ (western), central, and Çınarcık (eastern) basins on the Northern Anatolian Fault. The corrections are more uniformly distributed in the Black Sea off-the-shelf areas with a mean of around 270 mGal.

The seawater bathymetric stripping corrections mostly show a long-wavelength pattern over the land parts and it is almost constant possessing a mean value of 133 mGal and a low standard deviation of about 1.5 mGal (see Table 3). However, it produces significant variations onshore close to the coastlines and on some islands up to 163 mGal. The maximum values are seen over the southwest coasts of Turkey and on the islands located at the Hellenic trench. The central and the eastern coasts of the Black Sea region also exhibit higher variations above the mean value due to the narrower continental shelf. A more detailed assessment and interpretation of the computed quantities is beyond the scope of this study.

The results for the lake bathymetric stripping corrections are shown in Figure 5 and the statistics are presented in Table 4. It is evident from the figures that while the bathymetric stripping of lake waters has almost no effect on the surrounding lands outside a few kilometers

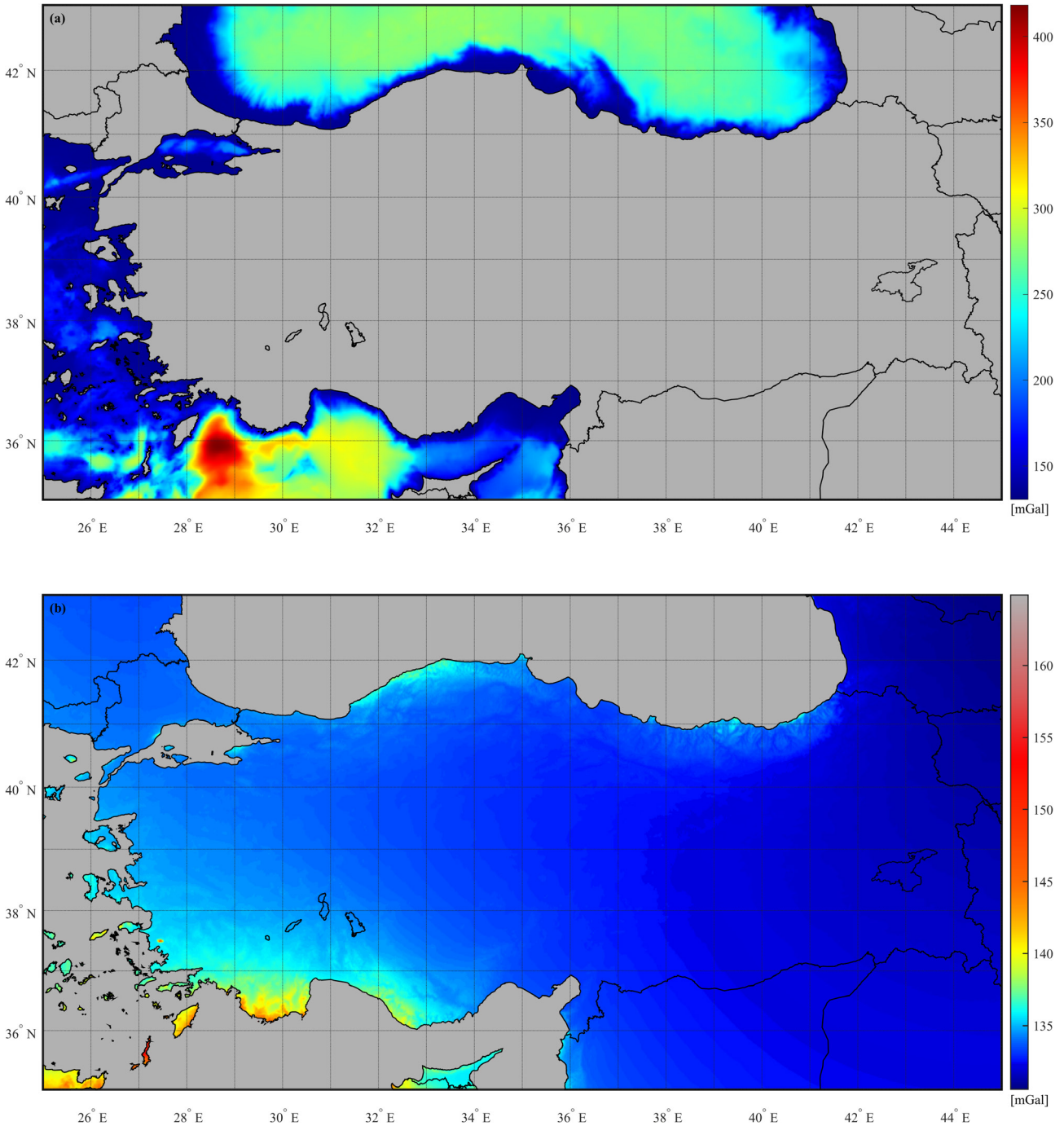

Figure 4. Global seawater gravity stripping effects in mGal unit. (a) offshore Turkey, (b) onshore Turkey.

Table 3. The statistics of the bathymetric stripping gravity corrections of global seawater around Turkey. Units are in mGal.

	Min	Max	Mean	Std
Offshore (sea part)	131.9	418.4	214.1	61.9
Onshore (land part)	130.6	163.1	133.1	1.5

width buffer zones around the lakes, it contributes considerably on the lake surfaces and over the buffer zones which should not be ignored in the microgravimetry applications. The water masses of Lake Van produce negative stripping corrections of up to 32 mGal over the deepest point at the southwest. There is a clear decreasing trend to the northeast and to the lakesides which follows

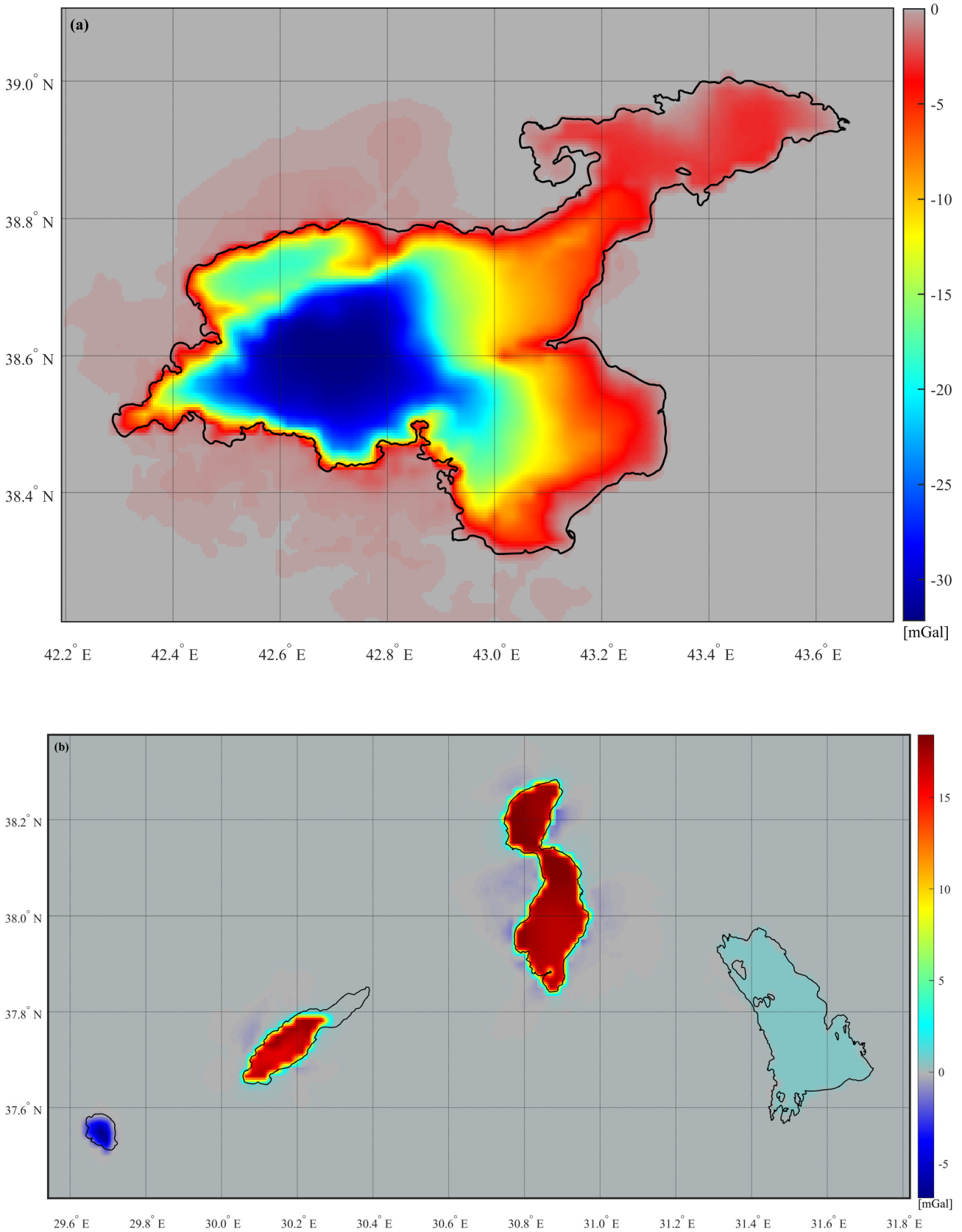

Figure 5. Lake water gravity stripping effects in mGal unit. (a) Lake Van, (b) Lakes Beyşehir, Eğirdir, Burdur, and Salda.

Table 4. The statistics of the bathymetric stripping gravity corrections of the five greatest lake water masses in Turkey. Statistics belong to the lake surfaces and their corresponding 1 km width buffer zones. Units are in mGal.

	Min	Max	Mean	Std
Lake Van	–32.158	–0.008	–11.017	10.092
Lake Beyşehir	–0.028	0.597	0.441	0.172
Lake Eğirdir	0.287	18.371	13.755	5.005
Lake Burdur	0.041	17.562	10.835	6.494
Lake Salda	–6.452	–0.106	–2.107	2.016

the bathymetry pattern and quickly vanishes outside the buffer zone. A mean positive bathymetric correction of around 0.5 mGal applies over the Lake Beyşehir surface due to its relatively shallower depth. The maximum corrections reach up to positive 18 mGal over the surfaces of Lakes Eğirdir and Burdur in which their distributions are almost constant with mean values of 14 mGal and 11 mGal, respectively. Lake Salda, one of the deepest inland lakes in Turkey, exhibits maximum bathymetric stripping corrections of about negative 6.5 mGal at its deepest point. Although 15 times smaller in size than Lake Beyşehir, its water masses produce 5 times larger density contrast gravity effects on the lake surface.

5. Conclusion

In this study, we first quantify the global ocean bathymetry-generated gravity stripping effects over Turkey for the geoscientists to correctly smooth the gravity field and unmask the gravitational signal of the sought anomalous masses. We apply the forward modelling method to compute the corrections on 1' × 1' arc-min grid points at the topographic surface using SRTM15+ global bathymetry and topography data and adopting a constant seawater density contrast of 1645 kgm^{-3}. It is found that the seawater stripping corrections mostly follow a long-wavelength pattern with a mean of 133 mGal over the mainland. Therefore, applying this correction in the inland locations further 100 km away from the nearest coastline will not contribute significantly to smooth the gravity field, because the observation points close to each other will have the same correction values. However, seawater density contrast produces remarkable high-frequency variations onshore close to the coasts, over marine areas, and on the islands up to 418 mGal which should be accounted for in the gravity data processing.

The second objective of this study is to determine the gravity stripping effects of the five largest and deepest inland lakes in Turkey, specifically the Lake Van to the east of Turkey and Lakes Beyşehir, Eğirdir, Burdur, and Salda located at the Lake District Region in south-western Turkey. As far as we know, this is the first work that shows the density contrast gravity effects of lake waters in Turkey. The lake bathymetry data acquired with a GNSS-aided high-precision echo sounder are provided by the Turkish General Directorate of Water Management. The water masses of these five lakes generate a considerable amount of gravity effects over the lake surfaces and their surrounding buffer zones of about 1 km width, which could reach up to tens of mGals at their deepest points.

It is strongly suggested that the bathymetric stripping gravity corrections of sea and lake waters be applied to the gravity data collected over the inland water bodies, coastal and offshore areas [e.g., airborne gravimetry described by Simav (2021)] especially when the data is being used for exploration purposes. We have utilized the constant seawater density instead of depth-dependent density model in the forward modelling of the bathymetric stripping corrections throughout the study. It should be noted that oceanographic models of salinity, temperature, and pressure can contribute to the more accurate computation of the gravitational field due to the depth-dependent seawater density variations. Finally, the bathymetry data of the other larger and deeper natural and man-made inland waters should be included in the further computations when their data are available.

Acknowledgment/disclaimer/conflict of interest

We thank to the Turkish General Directorate of Water Management for providing us the lake bathymetry data. The authors declare no conflict of interests. The MATLAB functions used in the computations can be shared upon request. Please contact the corresponding author at mehmet.simav@harita.gov.tr.

References

Asgharzadeh MF, von Frese RRB, Kim HR, Leftwich TE, Kim JW (2007). Spherical prism gravity effects by Gauss-Legendre quadrature integration. Geophysical Journal International 169: 1-11.

Becker JJ, Sandwell DT, Smith WHF, Braud J, Binder B et al. (2009). Global bathymetry and elevation data at 30 arc seconds resolution: SRTM30_PLUS. Marine Geodesy 32: 355-371.

Bielik M, Rybakov M, Lazar M (2013). Tutorial: The gravity-stripping process as applied to gravity interpretation in the eastern Mediterranean. The Leading Edge 32: 410.

Bomford G (1971). Geodesy. 3rd ed. Oxford: Clarendon Press.

D'Urso MG (2013). On the evaluation of the gravity effects of polyhedral bodies and a consistent treatment of related singularities. Journal of Geodesy 87: 239-252.

Grombein T, Seitz K, Heck B (2013). Optimized formulas for the gravitational field of a tesseroid. Journal of Geodesy 87: 645-660.

Groten E, Becker M (1995). Methods and experiences of high precision gravimetry as a tool for crustal movement detection. Journal of Geodynamics 19: 141-157.

Heiskanen WA, Moritz H (1967). Physical geodesy. San Francisco, CA, USA: W.H. Freeman and Company.

Hinderer J, Legros H, Crossley D (1991). Global earth dynamics induced gravity changes. Journal of Geophysical Research 96: 20257-20265.

Hinze WJ, Aiken C, Brozena J, Coakley B, Dater D et al. (2005). New standards for reducing gravity data: The North American gravity database. Geophysics 70: J25-J32.

Hinze WJ, von Frese RRB, Saad AH (2013). Gravity and magnetic exploration: Principles, practices and applications. New York: Cambridge University Press.

Hwang C, Hsu HJ, Chang ETY, Featherstone WE, Tenzer R et al. (2014). New free-air and Bouguer gravity fields of Taiwan from multiple platforms and sensors. Tectonophysics 611: 83-93.

Kuhn M, Seitz K (2005). Comparison of Newton's integral in the space and frequency domains. In: Sansò F, editor. A window on the future of geodesy. IAG symposia, vol 128. Springer, Berlin, pp. 386-391.

Kuhn M, Featherstone WE, Kirby JF (2009). Complete spherical Bouguer gravity anomalies over Australia. Australian Journal of Earth Sciences 56: 213-223.

Mazzotti S, Lambert A, Henton J, James T, Courtier N (2011). Absolute gravity calibration of GPS velocities and glacial isostatic adjustment in mid-continent North America. Geophysical Research Letters 38: L24311.

Mikuška J, Pašteka R, Marušiak I (2006). Estimation of distant relief effect in gravimetry. Geophysics 71: J59-J69.

Nagy D, Papp G, Benedek J (2000). The gravitational potential and its derivatives for the prism. Journal of Geodesy 74: 552-560.

Novák P (2000). Evaluation of gravity data for the Stokes-Helmert solution to the geodetic boundary-value problem. Technical Report, No. 207, UNB, Fredericton, Canada.

Novák P (2010). High resolution constituents of the Earth gravitational field. Surveys in Geophysics 31: 1-21.

Olson CJ, Becker JJ, Sandwell DT (2016). SRTM15_PLUS: Data fusion of Shuttle Radar Topography Mission (SRTM) land topography with measured and estimated seafloor topography. NCEI Accession 0150537.

Reguzzoni M, Sampietro D (2015). GEMMA: an Earth crustal model based on GOCE satellite data. International Journal of Applied Earth Observation and Geoinformation 35: 31-43.

Sandwell DT, Müller RD, Smith WHF, Garcia E, Francis R (2014). New global marine gravity model from CryoSat-2 and Jason-1 reveals buried tectonic structure. Science 346: 65-67.

Simav M, Yildiz H (2019). Evaluation of EGM2008 and latest GOCE based satellite only global gravity field models using densified gravity network: a case study in south-western Turkey. Bollettino di Geofisica Teorica ed Applicata 60: 49-68.

Simav M (2021). Results from the first strapdown airborne gravimetry campaign over the Lake District of Turkey. Survey Review. Volume: 53, Issue: 380, pp: 447-453. DOI: 10.1080/00396265.2020.1826140.

Simeoni O, Brueckl E (2009). Gravity stripping supports tectonic interpretation of the eastern Alps. Geophysical Research Abstracts 11: 7355.

Tenzer R, Hamayun K, Vajda P (2008a). Global secondary indirect effects of topography, bathymetry, ice and sediments. Contributions to Geophysics and Geodesy 38: 209-216.

Tenzer R, Hamayun K, Vajda P (2008b). Global map of the gravity anomaly corrected for complete effects of the topography, and of density contrasts of global ocean, ice, and sediments. Contributions to Geophysics and Geodesy 38: 357-370.

Tenzer R, Hamayun K, Vajda P (2009). Global maps of the CRUST 2.0 crustal components stripped gravity disturbances. Journal of Geophysical Research 114: 05408.

Tenzer R, Vajda P, Hamayun K (2010). A mathematical model of the bathymetry-generated external gravitational field. Contributions to Geophysics and Geodesy 40: 31-44.

Tenzer R, Gladkikh V, Novák P, Vajda P (2012a). Spatial and spectral analysis of refined gravity data for modelling the crust–mantle interface and mantle-lithosphere structure. Surveys in Geophysics 33: 817-839.

Tenzer R, Novák P (2012b). Bathymetric stripping corrections to gravity gradient components. Earth Planets Space 64: e21-e24.

Tenzer R, Novák P, Vladislav G (2012c). The bathymetric stripping corrections to gravity field quantities for a depth-dependent model of seawater sensity. Marine Geodesy 35: 198-220.

Timmen L (2010). Absolute and relative gravimetry. In: Xu G, editor. Sciences of geodesy-I: advances and future directions, Springer, Berlin, Germany, pp. 1-48.

Torge W (1989). Gravimetry. Berlin, Germany: Walter de Gruyter.

Tozer B, Sandwell DT, Smith WHF, Olson C, Beale JR et al. (2019). Global bathymetry and topography at 15 arcsec: SRTM15+. Earth and Space Science 6: 1847-1864.

Tsoulis D (2012). Analytical computation of the full gravity tensor of a homogeneous arbitrarily shaped polyhedral source using line integrals. Geophysics 77: F1–F11.

Uieda L, Barbosa VCF, Braitenberg C (2016). Tesseroids: Forward-modeling gravitational fields in spherical coordinates. Geophysics 81: F41-F48.

Vajda P, Vaníček P, Novák P, Meurers B (2004). On evaluation of Newton integrals in geodetic coordinates: Exact formulation and spherical approximation. Contributions to Geophysics and Geodesy 34: 289-314.

Vajda P, Vaníček P, Meurers B (2006). A new physical foundation for anomalous gravity. Studia Geophysica et Geodaetica 50: 189-216.

Vajda P, Ellmann A, Meurers B, Vaníček P, Novák P et al. (2008). Global ellipsoid referenced topographic, bathymetric and stripping corrections to gravity disturbance. Studia Geophysica et Geodaetica 52: 19-34.

Vajda P, Foroughi I, Vaníček P, Kingdon R, Santos M et al. (2020). Topographic gravimetric effects in earth sciences: Review of origin, significance and implications. Earth-Science Reviews 211: 103428.

van der Meijde M, Pail R, Bingham R, Floberghagen R (2015). GOCE data, models, and applications: A review. International Journal of Applied Earth Observation and Geoinformation 35: 4-15.

Vaníček P, Novák P, Martinec Z (2001). Geoid, topography, and the Bouguer plate or shell. Journal of Geodesy 75: 210-215.

Wild-Pfeiffer F, Heck B (2007). Comparison of the modelling of topographic and isostatic masses in the space and the frequency domain for use in satellite gravity gradiometry. In: Kılıçoğlu A, Forsberg R, editors. Proceedings of 1st international symposium of the IGFS. Gravity field of the Earth, Istanbul, Turkey, pp. 309-314.

Wild-Pfeiffer F (2008). A comparison of different mass elements for use in gravity gradiometry. Journal of Geodesy 82: 637-653.